ORIGINAL ARTICLE

Flexible ligand synthesis, characterization and liquid phase hydroxylation of phenol by H_2O_2 with host (nanopores of zeolite-Y)/guest $[VO([R]_2–N_2X_2)]^{2+}$ (R = H, CH$_3$; X = NH, O, S) nanocomposite materials

Masoud Salavati-Niasari

Abstract Encapsulation of Oxovanadium(IV) complexes of 12-membered macrocyclic ligands having N_2O_2, N_2S_2 and N_4 donor atoms in the nanocavity of zeolite-Y by the Flexible-Ligand Method (FLM) have been described. Oxovanadium(IV) complexes with macrocyclic ligands were entrapped in the nanocavity of zeolite-Y by a two-step process in the liquid phase: (i) adsorption of precursor ligand; 1,2-di(o-aminophenyl-, amino, oxo, thio)ethane, (N_2X_2); in the supercages of VO(IV)-Y; ($[VO(N_2X_2)]^{2+}$-Y (X = NH, O, S); and (ii) in situ condensation of the oxovanadium(IV) precursor complex with glyoxal or biacetyl; $[VO([R]_2–N_2X_2)]^{2+}$-Y (R = H, CH$_3$). The new Host–Guest Nanocomposite Materials (HGNM, $[VO([R]_2–N_2X_2)]^{2+}$-Y) have been characterized by FT-IR, DRS and UV–Vis spectroscopic techniques, XRD and elemental analysis, as well as nitrogen adsorption. Liquid-phase selective hydroxylation of phenol with H_2O_2 to a mixture of catechol and hydroquinone in CH$_3$CN has been reported using $[VO([R]_2–N_2X_2)]^{2+}$-Y as catalysts. Reaction conditions have been optimized by considering the concentration of substrate and oxidant, amount of catalyst, effect of time, volume of solvent and temperature. Under the optimized reaction conditions, $[VO([H]_2–N_4)]^{2+}$-Y gave 50.1% conversion of phenol after 6 h. All these catalysts are more selective toward catechol formation.

M. Salavati-Niasari (✉)
Institute of Nano Science and Nano Technology, University of Kashan, Kashan, P. O. Box. 87317-51167, Islamic Republic of Iran
e-mail: salavati@kashanu.ac.ir

M. Salavati-Niasari
Department of Chemistry, Faculty of Science, University of Kashan, Kashan, P. O. Box. 87317-51167, Islamic Republic of Iran

Introduction

One of the main targets of advanced organic synthesis is represented by the achievement of highly efficient, cheap and environmentally acceptable process. This result allows the formation of unwanted waste to be minimized, tedious and expensive purification procedures to be avoided. In the last decade, much effort has been paid to attach homogeneous transition metal complexes to insoluble supports, such as organic polymers or metal oxides. Reaction of transition metal complexes with solid surfaces may lead to stable solid catalysts, in which a transition-metal complex remains hooked or anchored to the surface atoms. These heterogenised catalysts may combine the ease of product separation with reactivity and selectivity founded with homogeneous catalysts [1–8].

Zeolites are crystalline aluminosilicates whose internal voids are formed by nanocavities and nanochannels of strictly regular dimensions and of different sizes and shapes. In particular, the structure of Y zeolite consists of almost spherical 1.3 nm cavities interconnected tetrahedrally through smaller apertures of 0.74 nm diameter. The metal complex can be easily accommodated inside the supercages of Y zeolite.

The term nanoporous materials have been used for those porous materials with pore diameters of less than 100 nm. Many kinds of crystallines and amorphous nanoporous materials such as framework silicates and metal oxides, zeolites, pillared clays, nanoporous silicon, carbon nanotubes and related porous carbons have been described

lately in the literature [1]. Nanopores encapsulated metal complexes are mostly used as heterogeneous and redox catalysts in petroleum industry and in the production of chemicals for various types of shape-selective conversion and separation reactions [9]. They form the basis of new environment-friendly technologies, involving cheaper, more efficient and more environment-friendly ways for carrying out chemical reactions. Transition metal-modified nanoporous molecular sieves with aluminosilicate frameworks catalyse a wide variety of synthetically useful oxidative transformations with clean oxidants such as H_2O_2 or O_2 under relatively mild conditions with the advantage of facile recovering and recycling, if compared to homogeneous liquid phase catalyst, like sulfuric acid [10–18].

The encapsulation of oxovanadium(IV) is widely used to modify the original properties of porous catalyst hosts in nanoporous structures. Both the acidity and redox properties can be modified by inserting oxovanadium(IV) into supercage of zeolite. Oxovanadium(IV)-containing nanoporous catalysts have been attracted considerable attention due to their remarkable activity in the catalytic [19–26]. In this paper, I described the preparation, physico-chemical characterization oxovanadium(IV) complexes of 12-membered macrocyclic ligand; 1,4-diaza,7,10-dioxo,5,6:11,12-dibenzo-[e,k]-cyclododeca-1,3-diene[N_2O_2]ane; [H]$_2$–N_2O_2, 2,3-dimethyl-1,4-diaza,7,10-dioxo,5,6:11,12-dibenzo-[e,k]-cyclododeca-1,3-diene[N_2O_2]ane; [CH$_3$]$_2$–N_2O_2, 1,4,7,10-tetraaza-5,6:11,12-dibenzo-[e,k]-cyclododeca-1,3-diene[N_4]ane; [H]$_2$–N_4, 2,3-dimethyl-1,4,7,10-tetraaza-5,6:11,12-dibenzo-[e,k]-cyclododeca-1,3-diene[N_4]ane; [CH$_3$]$_2$–N_4, 1,4-diaza,7,10-dithia,5,6:11,12-dibenzo-[e,k]-cyclododeca-1,3-diene[N_2S_2]ane; [H]$_2$–N_2S_2) and 2,3-dimethyl-1,4-diaza,7,10-dithia,5,6:11,12-dibenzo-[e,k]-cyclododeca-1,3-diene[N_2S_2]ane; [CH$_3$]$_2$–N_2S_2; encapsulated within the nanopores of zeolite-Y by the template condensation of glyoxal or biacetyl and precursor ligand; 1,2-di(o-aminophenyl-, amino, oxo, thio)ethane, N_2X_2; [VO([R]$_2$–N_2X_2)]$^{2+}$-Y (R = H, CH$_3$). Application of these complexes in the oxidation of phenol with H_2O_2 as oxygen donor has been shown. (Scheme 1, 2).

Experimental

Materials and physical measurements

Y-zeolite (Si/Al ∼ 2.53) was purchased from Aldrich (Lot No. 67812). All other reagents and solvent were purchased from Merck (pro-analysis) and dried using molecular sieves (Linde 4 Å). FT-IR spectra were obtained as KBr pellets in the range of 400–4,000 cm^{-1} with Shimadzu Varian 4300 spectrophotometer. The electronic spectra of the neat complexes were recorded on a Shimadzu UV–Vis scanning spectrometer (Model 2101 PC). Diffuse reflectance spectra (DRS) were registered on a Shimadzu UV/3101 PC spectrophotometer the range 1,500–200 nm, using MgO as reference. The elemental analysis (C, H and N) of the materials were performed using a Carlo ERBA Model EA 1108 analyzer. FAB mass spectra were recorded on a Kratos MS50TC spectrometer. ^{1}H-NMR spectra were obtained on a Bruker NMR 400 (400 MHz) spectrophotometer using CDCl$_3$ and (CD$_3$)$_2$SO as solvents. XRD patterns were recorded by a Rigaku D-max C III, X-ray diffractometer using Ni-filtered Cu Kα radiation. Nitrogen adsorption measurements were performed at 77 K using a Coulter Ofeisorb 100CX instrument. The samples were degassed at 150 °C until a vacuum better than 10^{-3} Pa was obtained. Micropore volumes were determined by the t-method, a "monolayer equivalent area" was calculated from the micropore volume [27, 28]. The stability of the encapsulated catalyst was checked after the reaction by UV–Vis and possible leaching of the complex was investigated by UV–Vis in the reaction solution after filtration of the zeolite. The amounts of oxovanadium(IV) complexes encapsulated in zeolite matrix were determined by the elemental analysis and by subtracting the amount of oxovanadium(IV) complex left in the solutions after the synthesis of the catalysts as determined by UV–Vis spectroscopy, from the amount taken for the synthesis. Atomic absorption spectra (AAS) were recorded on a Perkin-Elmer 4100–1319 Spectrophotometer using a flame approach, after acid (HF) dissolution of known amounts of the zeolitic material and SiO$_2$ was determined by gravimetric analysis.

Preparation of 1,2-di(o-nitrophenoxy)ethane

Ortho-nitrophenol (4.78 g) in hot dimethylformamide (5.0 mL) was treated slowly with potassium carbonate (2.39 g). The resulting solution was boiled gently and 1,2-dibromoethane (1.54 mL) was added dropwise with constant stirring for 30 min. The mixture was then refluxed gently for 2 h and concentrated under reduced pressure. On pouring the solution into cold water a granular yellow solid was filtered, washed with dilute aqueous NaOH, dried and recrystallized from glacial acetic acid, m.p. 169 °C, ^{1}H-NMR: (CDCl$_3$) δ 8.18 (2H, d), δ 7.35 (2H, m), δ 7.76 (2H, m), δ 7.08 (H, d), δ 4.08 (4H, O-CH$_2$) (Scheme 1).

Preparation of 1,2-di(o-aminophenyloxo)ethane

1,2-Di(o-nitrophenyloxo)ethane was heated under a nitrogen atmosphere with 5% Pd–C (0.5 g). N$_2$H$_4$ · H$_2$O (20.0 mL) was added in (5 mL) portions and the mixture refluxed until the solution become colourless (30 min). After filtration to remove the precipitate (if any), the
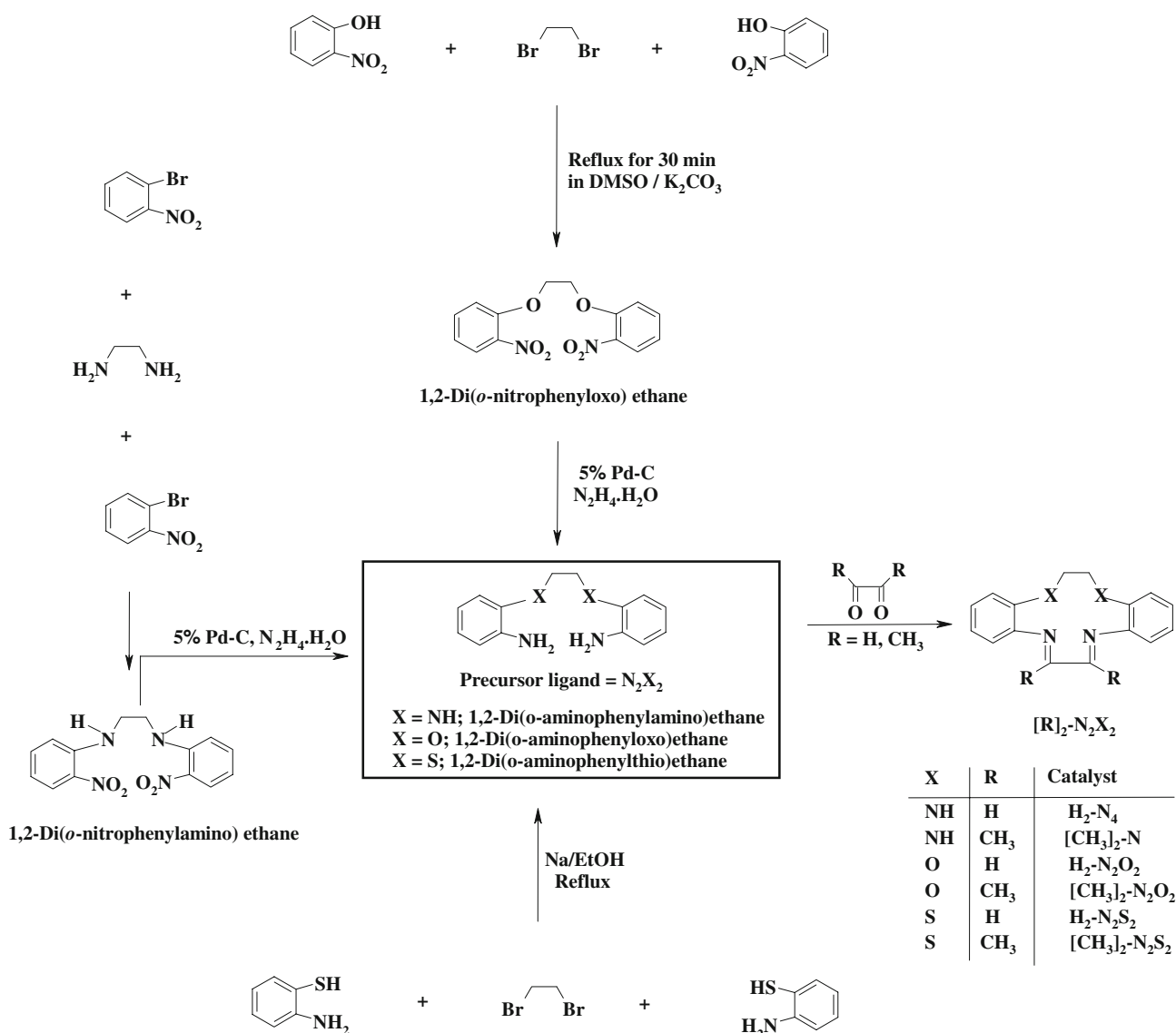
Scheme 1 Reaction rate for synthesis of 12-membered macrocyclic ligands

solution was evaporated to dryness and the solid residue recrystallized from hot ethanol under a nitrogen atmosphere. A residue of white plates was obtained. M.P. 131 °C. ^{1}H-NMR: (CDCl$_3$) δ 6.35 (2H, d), δ 7.16 (2H, m), δ 6.65 (2H, m), δ 7.08 (2H, d), δ 4.03 (4H, O-CH$_2$) (Scheme 1).

Preparation of 1,2-di(o-nitrophenylamino)ethane

1,2-Di(*o*-nitrophenylamino)ethane was prepared by heating BrC$_6$H$_4$NO$_2$ (2.0 g) with 1,2-diaminoethane (0.26 mL). The mixture was stirred rigorously until complete reaction had occurred. The heating was then reduced to keep the mass molten for a further use. The melt was poured into ethanol (50.0 mL), the solid so obtained was washed with a

mixture of diethyl ether (30.0 mL), benzene (30.0 mL) and 1 N NaOMe solution (10 mL). It was recrystallized from 1,2-dichloroethane give 1,2-di(*o*-nitrophenylamino)ethane (3.1 g) as bright orange needle shaped crystals. M.P. 193 °C. ^{1}H-NMR: (CDCl$_3$) δ 8.1 (2H, d), δ 7.33 (2H, m), δ 7.75 (2H, m), δ 7.06 (H, d), δ 4.07 (4H, NH–CH$_2$) (Scheme 1).

Preparation of 1,2-di(*o*-aminophenylamino)ethane

1,2-Di(*o*-nitrophenylamino)ethane was heated under a nitrogen atmosphere with 5% Pd–C (0.5 g). N$_2$H$_4$ · H$_2$O (20.0 mL) was added in (5 mL) portions and the mixture refluxed until the solution become colourless (30 min). After filtration to remove the precipitate (if any), the solution was
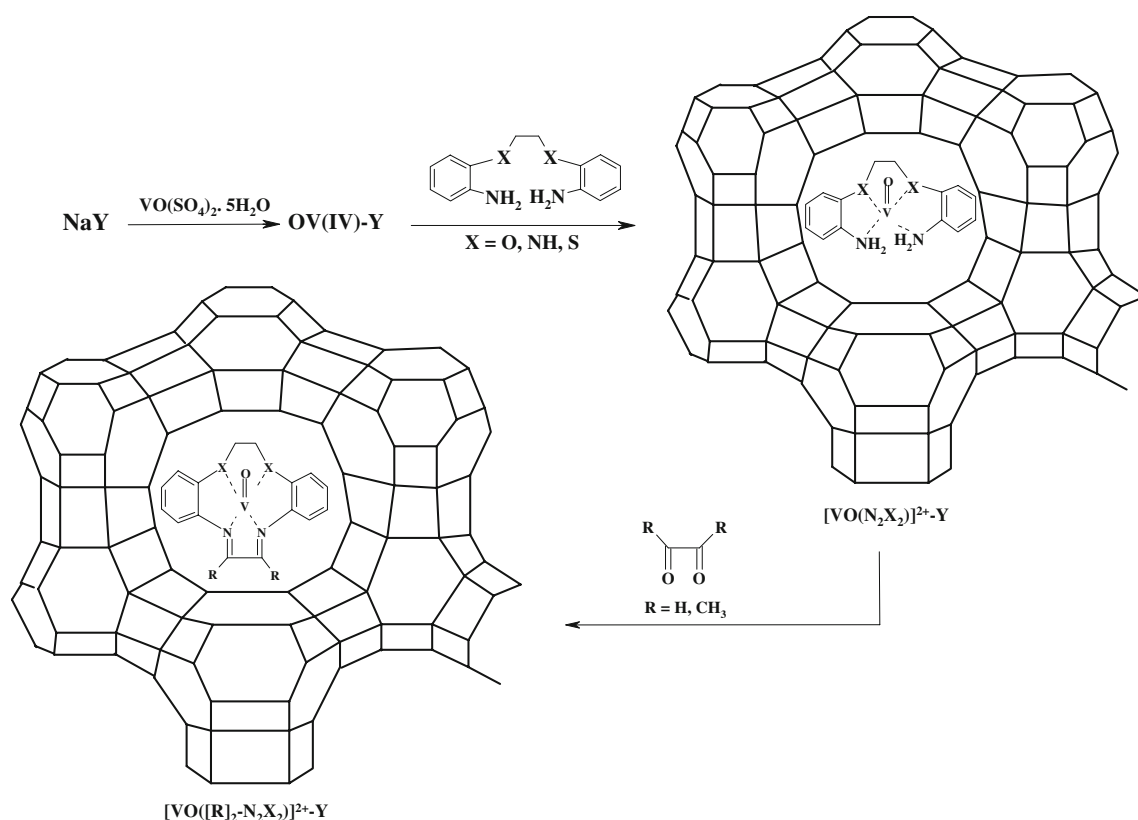
Scheme 2 Encapsulation of oxovanadium(IV) complexes of 12-membered macrocyclic ligands nanocomposite within the zeolite-Y

evaporated to dryness and the solid residue recrystallized from hot ethanol under a nitrogen atmosphere. A residue of white plates was obtained. M.P. 135 °C. ^{1}H-NMR: (CDCl$_3$) δ 6.36 (2H, d), δ 7.15 (2H, m), δ 6.65 (2H, d), δ 6.73 (2H, d), δ 3.04 (4H, m, NH–CH$_2$) (Scheme 1).

Preparation of 1,2-di(*o*-aminophenylthio)ethane (N$_2$S$_2$)

This diamine was prepared by heating *o*-HSC$_6$H$_4$NH$_2$ (1.09 g) with absolute (99%) ethanol (3 mL) containing sodium (0.201 g). 1,2-dibromoethane (0.372 mL) in ethanol (1 mL) was then added dropwise with constant stirring to the refluxing solution. The mixture was then cooled and poured into water (300 mL). The solid mass so obtained, was filtered, washed with water and dried. The product was recrystallized from ethanol, and a yellowish residue was obtained. M.P. 75 °C. ^{1}H-NMR: (CDCl$_3$) δ 6.35 (2H, d), δ 7.15 (2H, m), δ 6.63 (2H, m), δ 7.24 (2H, d), δ 2.88 (4H, m, S–CH$_2$) (Scheme 1).

Preparation of 12-membered macrocyclic ligands ([R]$_2$–N$_2$X$_2$, R = H, CH$_3$; X = NH, O, S)

1,4-diaza,7,10-dioxo,5,6:11,12-dibenzo-[*e,k*]-cyclododeca-1,3-diene[N$_2$O$_2$]ane; [H]$_2$–N$_2$O$_2$, 2,3-Dimethyl-1,4-diaza,

7,10-dioxo,5,6:11,12-dibenzo-[*e,k*]-cyclododeca-1,3-diene [N$_2$O$_2$]ane; [CH$_3$]$_2$–N$_2$O$_2$, 1,4,7,10-tetraaza-5,6:11,12-dibenzo-[*e,k*]-cyclododeca-1,3-diene[N$_4$]ane; [H]$_2$–N$_4$, 2,3-Dimethyl-1,4,7,10-tetraaza-5,6:11,12-dibenzo-[*e,k*]-cyclododeca-1,3-diene[N$_4$]ane; [CH$_3$]$_2$–N$_4$, 1,4-diaza,7,10-dithia,5,6:11,12-dibenzo-[*e,k*]-cyclododeca-1,3-diene[N$_2$S$_2$]ane; [H]$_2$–N$_2$S$_2$) and 2,3-Dimethyl-1,4-diaza,7,10-dithia,5,6:11,12-dibenzo-[*e,k*]-cyclododeca-1,3-diene[N$_2$S$_2$]ane; [CH$_3$]$_2$–N$_2$S$_2$ were obtained as described. To an ethanol solution (25 mL) of 0.05 mol glyoxal or biacetyl, an ethanol solution (25 mL) of precursor ligand; 1,2-di(*o*-aminophenyloxo)ethane, 1,2-di(*o*-aminophenylamino)ethane, 1,2-di(*o*-aminophenylthio)ethane (0.05 mol); was added in the presence of a few drops of *conc*. HCl and the resulting solution boiled under reflux for 8 h. The solution was then concentrated to half its volume under reduced pressure and kept overnight. The white/white off crystals which formed were filtered, washed with ethanol and dried under vacuum over P$_4$O$_{10}$. ^{1}H-NMR, (CDCl$_3$); [H]$_2$–N$_4$: δ 8.01 (2H, s), 6.93 (2H, d), d 7.14 (2H, m), 6.65 (2H, m), 6.76 (2H, d), 3.12 (4H, NH–CH$_2$); [CH$_3$]$_2$–N$_4$: δ 2.09 (6H, s), 6.92 (2H, d), d 7.13 (2H, m), 6.65 (2H, m), 6.75 (2H, d), 3.11 (4H, NH–CH$_2$); [H]$_2$–N$_2$O$_2$: δ 8.05 (2H, s), 6.92 (2H, d), d 7.12 (2H, m), 6.63 (2H, m), 6.74 (2H, d), 4.13 (4H, O–CH$_2$); [CH$_3$]$_2$–N$_2$O$_2$: δ 2.13 (6H, s), 6.91 (2H, d), d 7.12 (2H, m), 6.62 (2H, m), 6.73 (2H, d), 4.13 (4H, O–CH$_2$);

[H$_2$]–N$_2$S$_2$: δ 7.92 (2H, s), 6.90 (2H, d), d 7.11 (2H, m), 6.60 (2H, m), 6.72 (2H, d), 4.11 (4H, S–CH$_2$); [CH$_3$]$_2$–N$_2$S$_2$: δ 1.94 (6H, s), 6.90 (2H, d), d 7.10 (2H, m), 6.60 (2H, m), 6.72 (2H, d), 4.10 (4H, S–CH$_2$) (Scheme 1).

Preparation of neat complexes ([VO([R]$_2$–N$_2$X$_2$)](ClO$_4$)$_2$ (R = H, CH$_3$; X = NH, O, S)

The oxovanadium(IV) 12-membered macrocyclic complexes were prepared under ambient condition. To a hot solution of 12-membered macrocyclic ligand ([R]$_2$–N$_2$X$_2$); 2 mmol) in a mixed solvent (chloroform 20 and methanol 20 mL), a hot solution of VO(SO$_4$)$_2$ · 5H$_2$O (2 mmol) in methanol (15 mL) was added. The mixture was heated and a few drops of triethylamine were added. The reaction mixture was refluxed for 50 min. Excess lithium perchlorate dissolved in methanol was added to the filtrate, and the mixture was kept in the refrigerator until green solid formed. The solids were filtered, washed thoroughly with cold ethanol and dried in vacuum.

Preparation of VO(IV)-Y

An amount of 5.0 g of NaY zeolite was suspended in 300 mL of distilled water and to this was added VOSO$_4$ · 5H$_2$O (3.0 g, 12 mmol) with stirring. The reaction mixture was then heated with stirring at 90 °C for 24 h. The solid was filtered, washed with hot distilled water until the filtrate was free from any oxovanadium(IV) ion content, and dried for 12 h at 150 °C in air. The ionic exchange degree was determined by AAS.

Preparation of ([VO(N$_2$X$_2$)]$^{2+}$-Y (X = NH, S, O)

Encapsulated complex was performed with the Flexible Ligand Method (FLM). First, VO(IV)–Y was uniformly mixed with an excessive amount of precursor ligand (N$_2$X$_2$; 1,2-Di(o-aminophenyloxo)ethane, 1,2-Di(o-aminophenylamino)ethane, 1,2-Di(o-aminophenylthio)ethane) ($n_{\text{ligand}}/n_{\text{metal}} = 3$), and sealed into a round flask. The complexation was carried out under high vacuum conditions for 24 h at the temperatures of 150 °C. The uncomplexed ligands and the complex adsorbed on the exterior surface were removed by full Soxhlet extraction with ethanol. The extracted sample was ion-exchanged with 0.1 M NaCl aqueous solution to remove uncoordinated VO(IV) ions, followed by washing with deionized water until no Cl$^-$ anions could be detected with AgNO$_3$ aqueous solution. The products were dried at 150 °C for several hours.

Preparation of [VO([R]$_2$–N$_2$X$_2$)]$^{2+}$-Y (R = H, CH$_3$; X = NH, O, S)

To a stirred methanol suspension (100 mL) of precursor nanocatalyst ([VO(N$_2$X$_2$)]$^{2+}$-Y) (2 g) was slowly added glyoxal or biacetyl (under N$_2$ atmosphere). The mixture was heated under reflux condition for 24 h until a pale green suspension resulted. The solution was filtered and the resulting zeolites, were Soxhlet extracted with ethanol (for 4 h) and then with dichloromethane (for 4 h) to remove excess unreacted products from amine-carbonyl condensation and any VO(IV) complexes adsorbed onto the external surface of the zeolite crystallites. The resulting pale green solids were dried at 70 °C under vacuum for 12 h. The remaining precursor ions in zeolite were removed by exchanging with aqueous 0.1 M NaNO$_3$ solutions. The stability of the encapsulated catalyst was checked after the reaction by UV–Vis and possible leaching of the complex was investigated by UV–Vis in the reaction solution after filtration of the zeolite. The amounts of oxovanadium(IV) complexes encapsulated in zeolite matrix were determined by the elemental analysis and by subtracting the amount of oxovanadium(IV) complex left in the solutions after the synthesis of the catalysts as determined by UV–Vis spectroscopy, from the amount taken for the synthesis.

Hydroxylation of phenol

Catalytic experiments were carried out in a 50 mL reaction flask fitted with a water condenser. A general procedure was applied for all reactions. In a typical reaction, phenol (4.7 g, 0.05 mol) and 30% aqueous hydrogen peroxide (5.67 g, 0.05 mol) were mixed in 2 mL of MeCN and the reaction mixture was heated in an oil bath with continuous stirring at 80 °C. The catalyst to be tested (0.013 mmol) was added to it and the reaction was considered to begin. The reaction products were analyzed using a gas chromatograph after a specific interval of time by withdrawing a small aliquot. The effects of various parameters, such as hydrogen peroxide concentration (moles of H$_2$O$_2$ per mole of phenol), phenol concentration (moles of phenol per mole of H$_2$O$_2$), amount of catalyst, temperature, volume of MeCN solvent, etc., have been studied in detail for the catalyst [VO([H]$_2$–N$_4$)]$^{2+}$-Y; however, the basic procedure is the same as outlined above.

Results and discussion

Oxovanadium reacted with 12-membered macrocyclic ligands (1,4-diaza,7,10-dioxo,5,6:11,12-dibenzo-[e,k]-cyclododeca-1,3-diene[N$_2$O$_2$]ane; [H]$_2$–N$_2$O$_2$, 2,3-Dimethyl-1,

4-diaza,7,10-dioxo,5,6:11,12-dibenzo-[e,k]-cyclododeca-1, 3-diene[N₂O₂]ane; [CH₃]₂–N₂O₂, 1,4,7,10-tetraaza-5,6: 11,12-dibenzo-[e,k]-cyclododeca-1,3-diene[N₄]ane; [H]₂–N₄, 2,3-Dimethyl-1,4,7,10-tetraaza-5,6:11,12-dibenzo-[e,k]-cyclododeca-1,3-diene[N₄]ane; [CH₃]₂–N₄, 1,4-diaza,7,10-dithia,5,6:11,12-dibenzo-[e,k]-cyclododeca-1,3-diene[N₂S₂]ane; [H]₂–N₂S₂ and 2,3-Dimethyl-1,4-diaza,7,10-dithia,5,6:11,12-dibenzo-[e,k]-cyclododeca-1,3-diene[N₂S₂]ane; [CH₃]₂–N₂S₂) ligands in presence of LiClO₄ to yield the cationic complexes, [VO([R]₂–N₂X₂)]²⁺-Y (R = H, CH₃, X = NH, S, O) (Scheme 1). Acetonitrile solutions of these complexes were conductive (Table 1). Unfortunately, I could not grow any single crystals suitable for X-ray crystallographic studies. The molar conductance values of macrocyclic complexes (246–260 Ω^{-1} mol^{-1} cm^2) and measured correspond to 1:2 electrolytes.

The results of chemical analysis of the samples are given in Tables 1, 2. The parent NaY zeolite has Si/Al molar ratio of 2.53 which corresponds to a until cell formula [Na₅₆[(AlO₂)₅₆(SiO₂)₁₃₆]. The unit cell formula of metal-exchanged zeolites show a vanadium dispersion of 10.4 moles per unit cell (Na₃₄.₄(VO)₁₀.₄[(AlO₂)₅₆(SiO₂)₁₃₆] · nH₂O). The analytical data of each complex indicate V:C:N molar ratios "almost close to" those calculated for the mononuclear structure. The chemical compositions (Tables 1, 2) confirmed the purity and stoichiometry of the neat and of the zeolite-Y nanopore encapsulated complexes. The chemical analyses of the samples reveal the presence of organic matter with an C/N ratio roughly similar to that for neat complexes. The Si and Al contents in OV-Y and the zeolite complexes are almost in the same ratio as in the parent zeolite. This indicates little changes in the zeolite framework due to the absence of de-alumination in metal ion exchange.

The absence of absorption at ca. 3,400 cm^{-1} in the IR spectra of ligands shows that the free amino groups are absent, and the absence of a strong band at ca. 1,670–1,750 cm^{-1} shows the absence of ketonic groups. It confirms the elimination of water molecules and, as a result, cyclization takes places with formation of a macrocyclic ligand. In the IR spectra of [H]₂–N₂O₂ and [CH₃]₂–N₂O₂ (∼1,615 cm^{-1}), [H]₂–N₄ and [CH₃]₂–N₄ (∼1,620 cm^{-1}) and [H]₂–N₂S₂ and [CH₃]₂–N₂S₂ (∼1,605 cm^{-1}) a new band appears in all the ligands corresponding the $\upsilon(C = N)$ group. The IR spectra of these complexes show a moderate intensity absorption in the 1,590–1,614 cm^{-1} range attributed to the imine, $\upsilon(C = N)$ (Table 1). This moderate intensity absorption band is showing a shift to the lower side in the complexes, suggesting coordination through the nitrogen of the $\upsilon(C = N)$ group. The spectrum of ligand ([H]₂–N₄ and [CH₃]₂–N₄) shows a band at ∼3,310 cm^{-1}) corresponding to $\upsilon(N–H)$ [29]. On complexation this band is shifted towards the lower side 3,290 cm^{-1}. This

Table 1 Elemental analysis, vibrations parameters and some physical properties for ligands and 12-membered macrocyclic oxovanadium(IV) complexes

Complex	Calculated (found)					Λ_M^a, Ω^{-1} cm^2 mol^{-1}	μ_{eff} (MB)	IR (KBr, cm^{-1})			Important abs. bands (nm)^a			[V-ClO₄]$^+$	[V-2ClO₄]$^{2+}$
	C (%)	H (%)	N (%)	C/N	V (%)			$\upsilon_{C=N}$	υ_{N-H}	$\upsilon_{V=O}$	υ_{V-X}	$\upsilon_{V-N=}$		
[H]₂–N₄	72.70 (72.58)	6.10 (5.93)	21.20 (21.34)	3.43 (3.40)	–	–	–	1,620	3,310	–	–	–	–	–
[CH₃]₂–N₄	73.94 (73.79)	6.90 (6.79)	19.16 (19.28)	3.86 (3.83)	–	–	–	1,618	3,300	–	–	–	–	–
[H]₂–N₂O₂	72.16 (72.01)	5.30 (5.18)	10.52 (10.70)	6.86 (6.73)	–	–	–	1,615	–	–	–	–	–	–
[CH₃]₂–N₂O₂	73.45 (73.28)	6.16 (6.04)	9.52 (9.66)	7.72 (7.59)	–	–	–	1,613	–	–	–	–	–	–
[H]₂–N₂S₂	64.14 (64.00)	4.71 (4.59)	9.35 (9.50)	6.86 (6.74)	–	–	–	1,605	–	–	–	–	–	–
[CH₃]₂–N₂S₂	65.98 (65.76)	5.54 (5.40)	8.55 (8.69)	7.72 (7.72)	–	–	–	1,602	–	–	–	–	–	–
[VO([H]₂–N₄)](ClO₄)₂	36.25 (36.11)	3.04 (2.90)	10.57 (10.71)	3.43 (3.37)	9.61 (9.49)	260	1.73	1,615	3,300	975	–	460	575	475
[VO([CH₃]₂–N₄)](ClO₄)₂	38.73 (38.50)	3.61 (3.49)	10.04 (10.18)	3.86 (3.78)	9.13 (9.01)	255	1.72	1,610	3,295	971	427	456	602	504
[VO([H]₂–N₂O₂)](ClO₄)₂	36.11 (35.92)	2.65 (2.51)	5.26 (5.34)	6.86 (6.73)	9.57 (9.41)	257	1.74	1,616	–	976	433	462	577	477
[VO([CH₃]₂–N₂O₂)](ClO₄)₂	38.59 (38.40)	3.24 (3.10)	5.00 (5.18)	7.72 (7.41)	9.09 (8.91)	253	1.73	1,613	–	973	431	458	605	505
[VO([H]₂–N₂S₂)](ClO₄)₂	33.99 (33.81)	2.50 (2.39)	4.95 (5.09)	6.86 (6.64)	9.01 (8.88)	251	1.72	1,610	–	970	425	455	608	510
[VO([CH₃]₂–N₂S₂)](ClO₄)₂	36.43 (36.30)	3.06 (2.89)	4.72 (4.89)	7.72 (7.48)	8.58 (8.45)	246	1.71	1,605	–	967	420	450	637	537

^{a} In acetonitrile solutions

Table 2 Chemical composition and IR stretching frequencies (as KBr pellets) of nanopores of zeolite encapsulated 12-membered macrocyclic oxovanadium(IV) complexes

Sample	C (%)	H (%)	N (%)	C/N	Si (%)	Al (%)	Na (%)	V (%)	Si/Al	$v_{C=N}$ (cm^{-1})	d↔d (nm)
NaY	–	–	–	–	21.76	8.60	7.50	–	2.53	–	–
VO(IV)-Y	–	–	–	–	21.84	8.63	4.30	3.64	2.53	–	–
[VO([H]$_2$–N$_4$)]$^{2+}$-Y	3.96	2.63	1.23	3.21	20.50	8.10	5.72	2.40	2.53	1,613	551
[VO([CH$_3$]$_2$–N$_4$)]$^{2+}$-Y	3.98	2.69	1.10	3.62	20.44	8.08	5.70	2.39	2.53	1,608	554
[VO([H]$_2$–N$_2$O$_2$)]$^{2+}$-Y	3.95	2.65	0.59	3.64	20.53	8.11	5.71	2.41	2.53	1,614	549
[VO([CH$_3$]$_2$–N$_2$O$_2$)]$^{2+}$-Y	3.97	2.61	0.53	7.48	20.51	8.11	5.68	2.38	2.53	1,610	550
[VO([H]$_2$–N$_2$S$_2$)]$^{2+}$-Y	3.91	2.58	0.59	6.60	20.41	8.07	5.67	2.36	2.53	1,607	572
[VO([CH$_3$]$_2$–N$_2$S$_2$)]$^{2+}$-Y	3.93	2.62	0.53	7.43	20.46	8.08	5.65	2.35	2.53	1,600	575

indicates diversion of the electron cloud from the nitrogen of the imidazole or amino group, thus resulting in a lowering of the N–H stretching frequency. A partial list of IR spectral data of all catalysts is also presented in Tables 1, 2. The intensity of the peaks of the encapsulated complexes is weak due to the low concentration of the complexes in zeolite. The band due to $v(V = O)$ could not be located due to the appearance of a strong and broad band of the zeolite framework in the ~970 cm^{-1} region. Oxovanadium(IV) complexes with 12-membered macrocyclic ligands have green monomeric structures with square-pyramidal coordination or orange linear chain structures (···V = O···V = O···) with distorted octahedral coordination in the solid state. IR spectra of these complexes show the V = O stretching bands around 967–976 cm^{-1} for monomeric ones, and around 850–880 cm^{-1} for polymeric ones [30]. IR spectroscopy provides information on the integrity of the encapsulated complexes, as well as the crystallinity of the host zeolite. The IR bands of all heterogenised complexes are weak due to their low concentration in the zeolite. Oxovanadium(IV) complexes encapsulated in the zeolite nanopores did not show any significant shift in C = N stretching modes. We did not notice any appreciable changes in the frequencies of VO(IV)-complexes after incorporation into zeolite matrix.

The X-ray powder diffraction (XRD) patterns of NaY and VO(IV)-Y along with all encapsulated complexes were recorded at 2θ values between 10 and 70° to study their crystallinity. No significant variation were observed in the diffraction pattern during the encapsulation procedures which suggest that only little or negligible loss in crystallinity of the zeolite occurs.

The electronic spectra of all the complexes, in DMSO, show intraligand transition bands at 276 and 321 nm, while the MLCT bands fall near 375 nm. The position of the MLCT band depends on functional group. The electronic spectra of all nanocatalysts are collected in Tables 1, 2. As shown in the table, all complexes; [VO([R]$_2$–N$_2$X$_2$)]$^{2+}$, exhibit one broad band between 360 and 390 nm, which is assigned to a ligand to metal charge transfer (LMCT) transition. A weak band usually appears in the ~553 nm region in oxovanadium(IV) complexes [31]. This band is visible only for ([VO([R]$_2$–N$_2$X$_2$)]$^{2+}$-Y as a very weak band. Three spin-allowed transitions in the range 755–765, 468–484 and 553–571 nm are observed for the present complexes (Tables 1, 2), which are assigned to 2B$_2$ → E, 2B$_2$ → 2B$_1$ and 2B$_2$ → 2A$_1$ transitions, respectively, as expected for C$_{4V}$ symmetry [32]. Thus, IR and UV–Vis data indicate the encapsulation of oxovanadium(IV) complexes in the supercages of zeolite-Y. The diffuse reflectance spectra of oxovanadium(IV) complexes are almost identical before and after heterogenisation process, indicating that the complexes maintain their geometry and their electronic surrounding even after heterogenisation without significant distortion.

The surface area and pore volume of the catalysts are shown in Table 3. The inclusion of oxovanadium(IV) 12-membered macrocyclic complexes dramatically reduces the adsorption capacity and the surface area of the zeolite. It has been reported [33–37] that the BET surface area of X

Table 3 Surface area and pore volume data of 12-membered macrocyclic oxovanadium(IV) complexes encapsulated in nanopores of zeolite Y

Sample	Surface area (m^2/g)[a]	Pore volume (mL/g)[b]
NaY	545	0.31
VO(IV)-Y	516	0.29
[VO([H]$_2$–N$_4$)]$^{2+}$-Y	480	0.26
[VO([CH$_3$]$_2$N$_4$)]$^{2+}$-Y	477	0.25
[VO([H]$_2$–N$_2$O$_2$)]$^{2+}$-Y	482	0.26
[VO([CH$_3$]$_2$–N$_2$O$_2$)]$^{2+}$-Y	477	0.25
[VO([H]$_2$–N$_2$S$_2$)]$^{2+}$-Y	472	0.24
[VO([CH$_3$]$_2$–N$_2$S$_2$)]$^{2+}$-Y	466	0.23

[a] Surface area is the "monolayer equivalent area" calculated as explained in the Refs. [21, 22]

[b] Calculated by the *t*-method

Table 4 Hydroxylation of phenol to catechol and hydroquinone with H_2O_2 catalyzed by homogeneous oxovanadium(IV) 12-membered macrocyclic complexes in CH_3CN (Temperature, 80 °C; H_2O_2/phenol molar ratio, 1:1; Time (6 h)

Compound	Amount of catalyst (mmol)	Conversion (%)	Selectivity (%)	
			Catechol	Hydroquinone
$[VO([H]_2-N_4)](ClO_4)_2$	0.006	30.3	70.4	29.6
$[VO([H]_2-N_4)](ClO_4)_2$	0.013	38.7	76.3	23.7
$[VO([H]_2-N_4)](ClO_4)_2$	0.025	36.2	74.5	25.5
$[VO([H]_2-N_4)](ClO_4)_2$	0.050	30.9	70.3	29.7
$[VO([CH_3]_2-N_4)](ClO_4)_2$	0.013	32.6	63.6	36.4
$[VO([H]_2-N_2O_2)](ClO_4)_2$	0.013	34.8	68.5	31.5
$[VO([CH_3]_2-N_2O_2)](ClO_4)_2$	0.013	29.4	56.7	43.3
$[VO([H]_2-N_2S_2)](ClO_4)_2$	0.013	25.8	60.3	39.7
$[VO([CH_3]_2-N_2S_2)](ClO_4)_2$	0.013	19.6	52.4	47.6
$VOSO_4 \cdot 5H_2O$	0.013	10.6	53.9	46.1

Table 5 Hydroxylation of phenol to catechol and hydroquinone with H_2O_2 catalyzed by HGNM $(VO([R]_2-N_2X_2]^{2+}$-Y in CH_3CN (amount of catalyst: 0.013 mmol; temperature: 80 °C; H_2O_2/phenol molar ratio: 1:1; time: 6 h)

Compound	Conversion (%)	Selectivity (%)	
		Catechol	Hydroquinone
$[VO([H]_2-N_4)]^{2+}$-Y	50.1	85.7	14.3
$[VO([H]_2-N_4)]^{2+}$-Y[a]	49.3	84.5	15.5
$[VO([H]_2-N_4)]^{2+}$-Y[b]	48.8	83.7	16.3
$[VO([H]_2-N_4)]^{2+}$-Y[c]	47.9	83.1	16.9
$[VO([CH_3]_2-N_4)]^{2+}$-Y	46.4	73.4	26.6
$[VO([H]_2-N_2O_2)]^{2+}$-Y	47.2	75.2	24.8
$[VO([CH_3]_2-N_2O_2)]^{2+}$-Y	44.5	62.8	37.2
$[VO([H]_2-N_2S_2)]^{2+}$-Y	36.7	68.9	31.1
$[VO([CH_3]_2-N_2S_2)]^{2+}$-Y	32.5	59.1	40.9
NaY	3.9	46.0	54.0
VO(IV)-Y	16.7	60.6	39.4

[a] First reuse

[b] Second reuse

[c] Third reuse

Fig. 1 Hydroxylation products distribution in acetonitrile with neat complexes; $[VO([R]_2-N_2X_2)](ClO_4)_2/H_2O_2$

Fig. 2 Hydroxylation products distribution in acetonitrile with host–guest nanocatalyst
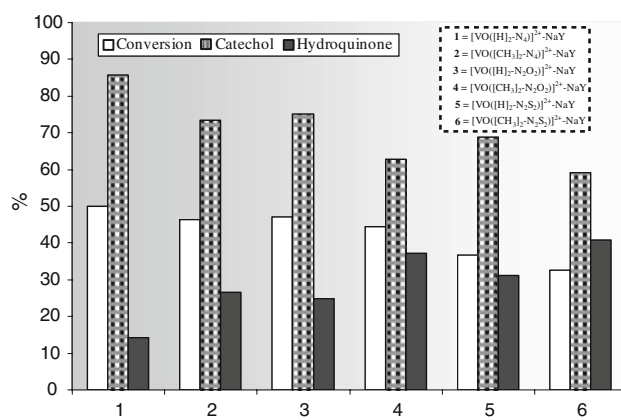
and Y zeolite containing phthalocyanine complexes are typically less than 100 $m^2 g^{-1}$. The lowering of the nanopore volume and surface area indicate the presence of 12-membered macrocyclic oxovanadium(IV) complexes within the nanocavities of the zeolites and not on the external surface.

The catalytic hydroxylation of phenol using $[VO([R]_2-N_2X_2]^{2+}$-Y (R = H, CH_3; X = NH, S, O) as catalysts and H_2O_2 as oxidant was studied (Tables 4, 5 and Figs. 1, 2). As the hydroxyl group of phenol is *ortho-* and *para-*directing, the oxidation of phenol is expected to give two major products, i.e., catechol and hydroquinone. The experimental results confirmed the presence of these two major products with a mass balance of >97%. Polymeric

material or other products, if any, present as minor constituents could not be detected by GC and were neglected. During catalytic oxidation, oxovanadium(IV) complexes react with H_2O_2 to give oxoperoxo complexes, which ultimately transfer oxygen to the substrate.

One of the major drawbacks of homogeneous metal complexes as catalysts is their irreversible deactivation due to formation of μ-oxo and μ-peroxo dimeric and other polymeric species especially when using oxidant. This problem may be avoided by isolating the metal X_2-haacac complexes from each other by encapsulation in the nanopores of a molecular sieve. The conversion increase by several orders of magnitude when the oxovanadium(IV) complexes are isolated from each other by encapsulation within the nanopore of the faujasite zeolites (Table 5 and Fig. 2).

The catalytic hydroxylation of phenol using the corresponding neat complexes as catalyst and H_2O_2 as oxidant in 2 mL CH_3CN have also been studied (Table 4 and Fig. 1). Interestingly, neat complexes have also shown good activity, though, conversion is lower as expected. The following general features were observed during this study: (1) the oxovanadium(IV) complexes containing electron donation (R = CH_3) are less active than their nonsubstituted analogs. (2) The zeolite-encapsulated complexes did not undergo any color change during the reaction and could be easily separated and reused many times. In contrast, the neat complexes, while they were active in the first cycle, were completely destroyed during the first run and changed color. (3) The $[R]_2$–N_2X_2 alone in the absence of metal were not catalytically active. (4) The activity of phenol hydroxylation decreases in the series $[VO([H]_2–N_4)]^{2+}$-Y > $[VO([H]_2–N_2O_2)]^{2+}$-Y > $[VO([CH_3]_2–N_4)]^{2+}$-Y > $[VO([CH_3]_2–N_2O_2)]^{2+}$-Y > $[VO([H]_2–N_2S_2)]^{2+}$-Y > $[VO([CH_3]_2–N_2S_2)]^{2+}$-Y. (5) The zeolites alone without the oxovanadium(IV) complexes were also catalytically inactive. Since the concentration of uncomplexed oxovanadium(IV) ions in the catalysts is also negligible, their contribution to catalytic activity may be neglected. Further evidence to confirm that the oxidation of cyclohexene is indeed catalysed to a significant extent by the solid zeolite catalyst containing the encapsulated oxovanadium(IV) complex and not by the free complex dissolved in solution was obtained as follows: In one set of two identical experiments, the solid catalyst; $[VO([H]_2–N_4)]^{2+}$-Y; was removed by centrifugation after a reaction time of 6 h. While the conversion of phenol proceeded further in the presence of the solid catalyst, there was no further conversion of phenol when the catalyst was removed from the reaction system. (6) The integrity of oxovanadium(IV) complexes encapsulated in the nanopores of zeolite-Y was confirmed by elemental, chemical analysis as well as spectroscopic studies. This was further supported by the fact that no leaching of oxovanadium(IV) ion was detected in the solution when a blank reaction was carried out (5.67 g H_2O_2 and 0.013 mmol catalyst in 2 mL CH_3CN at 80 °C).

The effect of amount of catalyst ($[VO([H]_2–N_4)]^{2+}$) on the hydroxylation reaction is illustrated in Table 4. Among

three different amounts (e.g., 0.006, 0.013, 0.025 and 0.050 mmol) of catalyst an amount of 0.013 mmol gave almost comparable results for the fixed amount of oxidant and substrate in 2 mL of MeCN. Thus, 0.013 mmol of catalyst is sufficient to give its best performance.

Table 5 and Fig. 2 presents all these data along with percent selectivity for the formation of catechol and hydroquinone. The presence of these two products was also observed with a mass balance of about 97% when phenol was catalysed by $[VO([H]_2–N_4)]^{2+}$-Y encapsulated in the nanopore of zeolite-Y using H_2O_2 as an oxidant. On increasing the reaction time from 6 to 12 h (Fig. 3), only minor increase in the transformation of phenol as well as percent selectivity for the formation of catechol and hydroquinone were observed for $[VO([H]_2–N_4)]^{2+}$-Y catalyst. At the end of the reaction, the catalyst was separated by filtration, thoroughly washed with solvent and reused under similar conditions. Although the analysis of the recovered catalysts by AAS showed no reduction in the amount of metal ions, they showed a slightly lower catalytic activity (0.5%, Table 5).

The results in Fig. 4 show the effect of H_2O_2 concentration on the phenol oxidation reaction. Four different molar ratios of oxidant to phenol were used (1:1, 2:1, 0.5:1, 0.33:1, 1:2 mol) in which the amount of phenol was kept fixed at 4.7 g (0.05 mol) in 2 mL of CH_3CN. The percentage phenol conversion also increased with the increase of H_2O_2 to phenol ratio. The reason for increasing may be due to the dilution of the reaction mixture by the presence of larger amount of water molecules in H_2O_2 solution. This result shows that large H_2O_2 concentration is not an essential condition to maximize phenol transformation. While keeping parameters such as amount of catalyst (0.013 mmol), volume and type of solvent (2 mL CH_3CN) and amount of oxidant (5.67 g) fixed, the catalytic reaction was performed using four different molar ratios of phenol
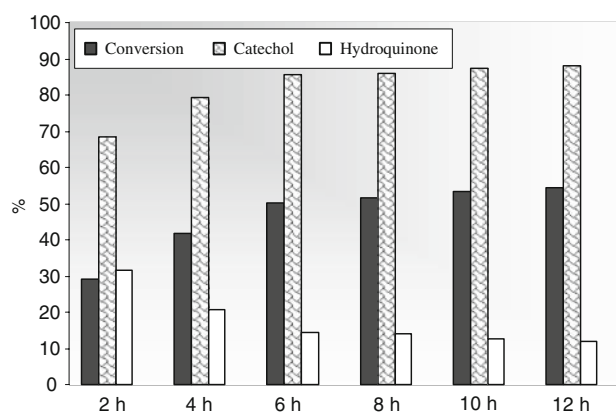
Fig. 3 Effect of time on hydroxylation of phenol with H_2O_2 (catalyst: $[VO([H]_2–N_4)]^{2+}$-Y; solvent: CH_3CN; amount of catalyst: 0.013 mmol; temperature: 80 °C; H_2O_2/phenol molar ratio: 1:1)
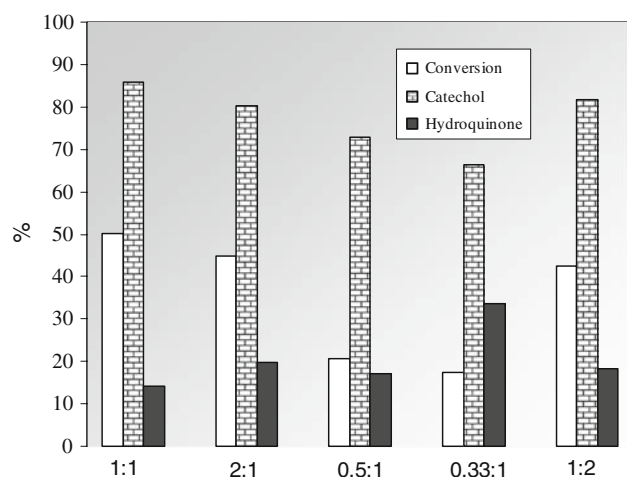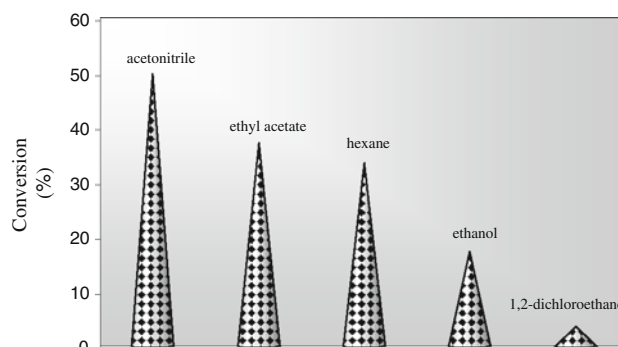
Fig. 4 Effect of H_2O_2/phenol molar ratio on hydroxylation of phenol (catalyst: $[VO([H]_2–N_4)]^{2+}$-Y; solvent: CH_3CN; amount of catalyst: 0.013 mmol; temperature: 80 °C; time: 6 h)

Table 6 Effect of solvent on hydroxylation of phenol (catalyst: $[VO([H]_2–N_4)]^{2+}$-Y; amount of catalyst: 0.013 mmol; temperature: 80 °C; time: 6 h; H_2O_2/phenol molar ratio: 1:1)

Solvent	Conversion (%)	Selectivity (%)	
		Catechol	Hydroquinone
Acetonitrile	50.1	85.7	14.3
Ethyl acetate	37.4	80.6	19.4
Hexane	33.6	74.5	25.5
Ethanol	17.5	66.3	33.7
1,2-Dichloroethane	3.8	54.9	45.1

to H_2O_2 at 80 °C, maximum conversion was observed with 1:1 molar ratio. Increasing or decreasing the concentration of phenol beyond this molar ratio under the same reaction conditions led to lower conversions.

The effect of various solvents for the hydroxylation of phenol with $[VO([H]_2–N_4)]^{2+}$-Y catalyst was also studied (Table 6; Fig. 5). In the present study, five different solvents viz. acetonitrile, ethyl acetate, hexane, ethanol and 1,2-dichloroethane were used to see their effect on the conversion. Although it is difficult to explain here as to which property of the solvent influenced the phenol conversion most, it is clear from the results that CH_3CN is the best solvent. The maximum percent phenol conversion obtained with various solvents is in the order, CH_3CN (50.1%) > ethyl acetate (37.4%) > hexane (33.6%) > ethanol (17.5%) > 1,2-dichloroethane (3.8%). It was also discovered that 2 mL of CH_3CN was found to be sufficient to perform the reaction to give best result. Increasing the amount of solvent, the catalytic reaction always led to reduced performance. A decreased solvent amount (1 mL) was found insufficient to dissolve the substrate and formed a non-homogeneous reaction mixture.

Fig. 5 Hydroxylation of phenol with hydrogen peroxide in various solvent with $[VO([H]_2–N_4)]^{2+}$-Y (solvent: CH_3CN; amount of catalyst: 0.013 mmol; temperature: 80 °C; time: 6 h; H_2O_2/phenol molar ratio: 1:1)
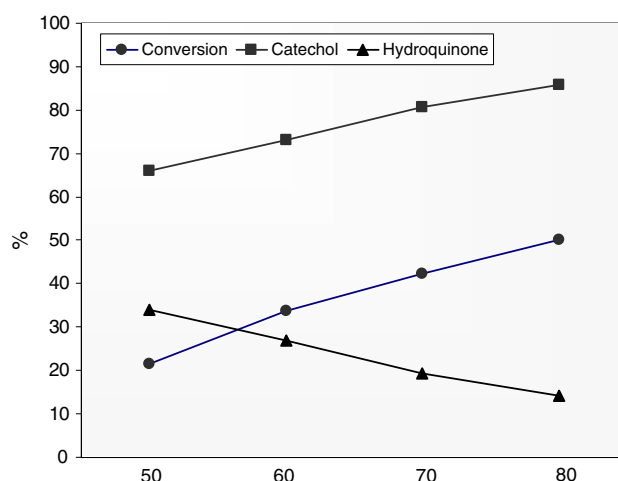
Fig. 6 Effect of temperature on hydroxylation of phenol (catalyst: $[VO([H]_2–N_4)]^{2+}$-Y; solvent: CH_3CN; amount of catalyst: 0.013 mmol; time: 6 h; H_2O_2/phenol molar ratio: 1:1)

Temperature of the reaction also has influence on the performance of the catalyst for phenol conversion (Fig. 6). Four different temperatures (50, 60, 70 and 80 °C) were used while keeping other parameters fixed (i.e., 0.013 mmol of $[VO([H]_2–N_4)]^{2+}$-Y), 5.67 g H_2O_2 and 4.7 g phenol) for the catalytic tests in 2 mL of CH_3CN. The conversion of the catalyst was found to increase as the temperature was raised from 50 to 80 °C.

Catalyst $[VO([H]_2–N_4)]^{2+}$-Y shows the highest conversion of 50.1%. It is interesting to note that even VO(IV)-Y has catalytic activity comparable with that of $[VO([H]_2–N_4)]^{2+}$-Y. However, for VO(IV)-Y leaching of the oxovanadium(IV) ion is always possible. Increasing the reaction time from 6 to 24 h does not show any appreciable change in hydroxylation products. Figure 3 gives data for phenol conversion along with the selectivity of catechol and hydroquinone formation for these catalysts after 2–12 h of reaction time.

The results clearly suggest that $[VO([H]_2–N_4)]^{2+}$-Y efficiently catalyses conversion of phenol to catechol with 85.7% selectivity. The greater activity of $[H]_2–N_4$ system has clearly arisen from the existence of electron donating ligand which facilitate the electron transfer rate, a process that has previously observed by us in other oxidation reactions [30]. All conversions efficiencies with high selectivity obtained in this study are significantly higher than that obtained using oxovanadium(IV) Schiff-base complexes [38].

Conclusion

In summary, the results show that $[VO([R]_2–N_2X_2)]^{2+}$-Y (R = H, CH$_3$; X = NH, O, S) can be encapsulated in the nanopores of zeolite. 12-Membered macrocyclic oxovanadium(IV) complexes were entrapped in the nanocavity of zeolite-Y by a two-step process in the liquid phase: (i) adsorption of precursor ligand (1,2-di(o-aminophenyl-, amino, oxo, thio)ethane; N_2X_2) in the supercages of the zeolite, and (ii) in situ condensation of the oxovanadium(IV) precursor complex with glyoxal or biacetyl ($[VO([R]_2–N_2X_2)]^{2+}$-Y (R = H, CH$_3$; X = NH, O, S). This strategy appears to be effective for the encapsulated of oxovanadium(IV) complexes with tetradentate 12-membered macrocyclic ligand. Furthermore, the spectroscopic data suggests that the encapsulated complexes experience very little distortion in the supercage and that the chemical ligation to the zeolite surface is minimal. Phenol was catalytically oxidized in the presence of H$_2$O$_2$ (5.5 g) and host–guest nanocomposite (0.013 mmol) in 2 mL of MeCN at 80 °C, affording catechol and hydroquinone with good catechol selectivity. Under the same reaction conditions the catalytic activity of these complexes follow the order: $[VO([H]_2–N_4)]^{2+}$-Y > $[VO([H]_2–N_2O_2)]^{2+}$-Y > $[VO([CH_3]_2–N_4)]^{2+}$-Y > $[VO([CH_3]_2–N_2O_2)]^{2+}$-Y > $[VO([H]_2–N_2S_2)]^{2+}$-Y > $[VO([CH_3]_2–N_2S_2)]^{2+}$-Y after 6 h of reaction time (Fig. 2). The effect of temperature, type of solvents, amount of nanocatalyst, oxidant used on the catalytic activity and product selectivity were discussed. Neat complexes are also good catalysts but result in considerably less conversion of phenol in comparison to encapsulated one. Comparable IR spectral patterns of fresh and used encapsulated catalysts suggest that these can be used further for catalytic study.

References

1. Vos, D.E., Vankelecom, I.F.J., Jacobs, P.A. (eds.): Chiral Catalyst Inmobilization and Recycling. Wiley, Weinheim (2000)

2. Gevers, L.E.M., Vankelecom, I.F.J., Jacobs, P.A.: Solvent-resistant nanofiltration with filled polydimethylsiloxane (PDMS) membranes. J. Membr. Sci. **278**, 199–204 (2006). doi:10.1016/j.memsci.2005.10.056

3. Langhendries, G., Baron, G.V., Vankelecom, I.F.J., Parton, R.F., Jacobs, P.A.: Selective hydrocarbon oxidation using a liquid-phase catalytic membrane reactor. Catal. Today **56**, 131–135 (2000). doi:10.1016/S0920-5861(99)00269-2

4. Knops-Gerrits, P.P., Vankelecom, I.F.J., Béatse, E., Jacobs, P.A.: Epoxidation of olefines with PDMS membranes containing zeolite occluded manganese diimine complexes. Catal. Today **32**, 63–70 (1996). doi:10.1016/S0920-5861(96)00179-4

5. Parton, R.F., Vankelecom, I.F.J., Tas, D., Janssen, K.B.M., Knops-Gerrits, P.P., Jacobs, P.A.: Membrane occluded catalysts: a higher order mimic with improved performance. J. Mol. Catal. Chem. **113**, 283–292 (1996). doi:10.1016/S1381-1169(96)00091-X

6. Vankelecom, I.F.J., Parton, R.F., Casselman, M.J.A., Uytterhoeven, J.B., Jacobs, P.A.: Oxidation of cyclohexane using FePcY-zeozymes occluded in polydimethylsiloxane membranes. J. Catal. **163**, 457–464 (1996). doi:10.1006/jcat.1996.0347

7. Schüth, F., Schmidt, W.: Microporous and mesoporous materials. Adv. Mater. **14**, 629–638 (2002). doi:10.1002/1521-4095(20020503)14:9<629::AID-ADMA629>3.0.CO;2-B

8. Schuth, F., Sing, K., Weitkamp, J. (eds.): Handbook of Porous Solids, vol. I–V. Wiley-VCH, Weinheim (2002)

9. Kaucky, D., Vondrova, A., Dedecek, J., Wichterlova, B.: Activity of Co ion sites in ZSM-5, ferrierite, and mordenite in selective catalytic reduction of NO with methane. J. Catal. **194**, 318–329 (2000). doi:10.1006/jcat.2000.2925

10. Połtowicz, J., Pamin, K., Tabor, E., Haber, J., Adamski, A., Sojka, Z.: Metallosalen complexes immobilized in zeolite NaX as catalysts of aerobic oxidation of cyclooctane. Appl. Catal. Gen. **299**, 235–242 (2006). doi:10.1016/j.apcata.2005.10.034

11. Jacob, C.R., Verkey, S.P., Ratnasamy, P.: Selective oxidation over copper and manganese salens encapsulated in zeolites. Microporous Mesoporous Mater. **22**, 465–474 (1998)

12. Chen, P., Fan, B., Song, M., Jin, C., Ma, J., Li, R.: Zeolite-encapsulated Ru(III) tetrahydro-Schiff base complex: an efficient heterogeneous catalyst for the hydrogenation of benzene under mild conditions. Catal. Commun. **7**, 969–973 (2006)

13. Jin, C., Fan, W., Jia, Y., Fan, B., Ma, J., Li, R.: Encapsulation of transition metal tetrahydro-Schiff base complexes in zeolite Y and their catalytic properties for the oxidation of cycloalkanes. J. Mol. Catal. A: Chem. **249**, 23–30 (2006)

14. Knopsgerrits, P.P., De vos, D., Thibaultstarzyk, F., Jacobs, P.A.: Zeolite-encapsulated Mn(II) complexes as catalysts for selective alkene oxidation. Nature **369**, 543–546 (1994)

15. Balkus Jr., K.J., Khanrnamedova, A.K., Dixon, K.M., Bedioui, F.: Oxidations catalyzed by zeolite ship-in-a-bottle complexes. Appl. Catal. A: Gen. **143**, 159–173 (1996)

16. Salavati-Niasari, M., Davar, F.: Host (nanodimensional pores of zeolite Y)-guest (3, 10-dialkyl-dibenzo-1, 3, 5, 8, 10, 12-hexaazacyclotetradecane, [Ni(R2Bzo2[14]aneN6)]2 +) nanocomposite materials: synthesis, characterization and catalytic oxidation of cyclohexene. Inorg. Chem. Commun. **9**, 263–268 (2006)

17. Salavati-Niasari, M.: Host (nanocavity of zeolite-Y)-guest (tetraaza[14]annulene copper(II) complexes) nanocomposite materials: synthesis, characterization and liquid phase oxidation of benzyl alcohol. J. Mol. Catal. A: Chem. **245**, 192–199 (2006)

18. Salavati-Niasari, M., Davar, F.: In situ one-pot template synthesis (IOPTS) and characterization of copper(II) complexes of 14-membered hexaaza macrocyclic ligand "3, 10-dialkyl-dibenzo-1, 3, 5, 8, 10, 12 hexaazacyclotetradecane". Inorg. Chem. Commun. **9**, 175–179 (2006)

19. Joseph, T., Srinivas, D., Gopinath, C.S., Halligudi, S.B.: Spectroscopic and catalytic activity studies of VO(Saloph) complexes

encapsulated in zeolite-Y and Al-MCM-41 molecular sieves. Catal. Lett. **83**, 209–214 (2002)

20. Bowers, C., Dutta, P.K.: Olefin oxidation by zeolite-encapsulated Mn(salen)$^+$ complexes under ambient conditions. J. Catal. **122**, 271–279 (1990)

21. Paez-Mozo, E., Gabriunas, N., Maggi, R., Acosta, D., Ruiz, P., Delmon, B.: Selective olefin oxidation with cobalt phthalocyanine encapsulated in Y-zeolite. J. Mol. Catal. **91**, 251–258 (1994)

22. Raja, R., Ratnasamy, P.: Selective oxidation of phenols using copper complexes encapsulated in zeolites. Appl. Catal. A: Gen. **143**, 145–158 (1996)

23. Jacob, C.R., Varkey, S.P., Ratnasamy, P.: Oxidation of para-xylene over zeolite-encapsulated copper and manganese complexes. Appl. Catal. A: Gen. **182**, 91–96 (1999)

24. Maurya, M.R., Titinchi, S.J.J., Chand, S.: Spectroscopic and catalytic activity study of N, N′-bis(salicylidene)propane-1, 3-diamine copper(II) encapsulated in zeolite-Y. Appl. Catal. A: Gen. **228**, 177–187 (2002)

25. Alvarez, H.M., Malta, L.F.B., Herbst, M.H., Horn Jr., A., Antunes, O.A.C.: Catalytic isosafrol oxidation mediated by impregnated and encapsulated vanadyl-Y-zeolite under microwave irradiation. Appl. Catal. A: Gen. **326**, 82–88 (2007)

26. Maurya, M.R., Chandrakar, A.K., Chand, Sh.: Zeolite-Y encapsulated metal complexes of oxovanadium(VI), copper(II) and nickel(II) as catalyst for the oxidation of styrene, cyclohexane and methyl phenyl sulfide. J. Mol. Catal. A: Chem. **274**, 192–201 (2007)

27. Salavati-Niasari, M.: Ship-in-a-bottle synthesis, characterization and catalytic oxidation of styrene by host (nanopores of zeolite-Y)/guest ([bis(2-hydroxyanil)acetylacetonato manganese(III)]) nanocomposite materials (HGNM). Microporous Mesoporous Mater. **95**, 248–256 (2006)

28. Lineares-Solano, A.: Textural characterization of porous carbons by physical adsorption of gases. In: Figueiredo, J.L., Moulijn, J.A. (eds.) Carbon and coal gasification, pp. 137–187. M. Nijhoff, MA, Dordrecht (1986)

29. Singh, P.K., Koacher, J.K., Tondan, J.P.: Boron complexes of some oxygen-nitrogen and sulphur-nitrogen containing chelating agents. J. Inorg. Nucl. Chem. **43**, 1755–1758 (1981)

30. Mathew, M., Carty, A.J., Palenik, G.J.: Unusual complex containing bridging vanadyl groups. Crystal structure of N, N′-propylenebis(salicylaldiminato)oxovanadium(IV). J. Am. Chem. Soc. **92**, 3197–3198 (1970)

31. Ballhausen, C.J., Gray, H.B.: Molecular Orbital Theory. Benjamin, New York (1965)

32. Salavati-Niasari, M., Ganjali, M.R., Norouzi, P.: Host (nanopores of zeolite Y)-guest (oxovanadium(IV) tetradentate Schiff-base complexes) nanocomposite materials: synthesis, characterization and liquid phase hydroxylation of phenol with hydrogen peroxide. J. Porous Mater. **14**, 423–432 (2007)

33. Salavati-Niasari, M.: Synthesis and characterization of host (nanodimensional pores of zeolite-Y)–guest [unsaturated 16-membered octaaza–macrocycle manganese(II), cobalt(II), nickel(II), copper(II), and zinc(II) complexes] nanocomposite materials. Chem. Lett. **34**, 1444–1445 (2005)

34. Salavati-Niasari, M.: Nanoscale microreactor-encapsulation of 16-membered hexaaza macrocycle nickel(II) complexes: in situ one-pot template synthesis (IOPTS), characterization and catalytic activity. Microporous Mesoporous Mater. **92**, 173–180 (2006)

35. Salavati-Niasari, M., Davar, F.: Synthesis, characterization and catalytic activity of copper(II) complexes of 14-membered macrocyclic ligand; 3, 10-dialkyl-dibenzo-1, 3, 5, 8, 10, 12-hexaazacyclotetradecanel/zeolite encapsulated nanocomposite materials. Inorg. Chem. Commun. **9**, 304–309 (2006)

36. Salavati-Niasari, M., Shakouri-Arani, M., Davar, F.: Flexible ligand synthesis, characterization and catalytic oxidation of cyclohexane with host (nanocavity of zeolite-Y)/guest (Mn(II), Co(II), Ni(II) and Cu(II) complexes of tetrahydro-salophen) nanocomposite materials. Microporous Mesoporous Mater. **116**, 77–85 (2008)

37. Salavati-Niasari, M.: Nanoscale microreactor-encapsulation 14-membered nickel(II) hexamethyl tetraaza: synthesis, characterization and catalytic activity. J. Mol. Catal. A: Chem. **229**, 159–164 (2005)

38. Salavati-Niasari, M., Elzami, M.R., Mansournia, M.R., Hydarzadeh, S.: Alumina-supported vanadyl complexes as catalysts for the C-H bond activation of cyclohexene with *tert*-butylhydroperoxide. J. Mol. Catal. A **221**, 169–175 (2004)